Applied Physics Letters ARTICLE scitation.org/journal/apl

Epitaxial niobium nitride superconducting nanowire single-photon detectors

Cite as: Appl. Phys. Lett. **117**, 132601 (2020); doi: 10.1063/5.0018818
Submitted: 17 June 2020 · Accepted: 15 September 2020 ·
Published Online: 28 September 2020

Risheng Cheng,[1] John Wright,[2] Huili G. Xing,[2,3,4] Debdeep Jena,[2,3,4,a)] and Hong X. Tang[1,b)]

AFFILIATIONS

[1]Department of Electrical Engineering, Yale University, New Haven, Connecticut 06511, USA
[2]Department of Materials Science and Engineering, Cornell University, Ithaca, New York 14853, USA
[3]School of Electrical and Computer Engineering, Cornell University, Ithaca, New York 14853, USA
[4]Kavli Institute for Nanoscale Science, Cornell University, Ithaca, New York 14853, USA

[a)]Electronic mail: djena@cornell.edu
[b)]Author to whom correspondence should be addressed: hong.tang@yale.edu

ABSTRACT

Superconducting nanowires used in single-photon detectors have been realized on amorphous or poly-crystalline films. Here, we report the first use of single-crystalline NbN thin films for superconducting nanowire single-photon detectors (SNSPDs). Grown by molecular beam epitaxy (MBE) at high temperature on nearly lattice-matched AlN-on-sapphire substrates, the NbN films exhibit a high degree of uniformity and homogeneity. Even with relatively thick films, the fabricated nanowire detectors show saturated internal efficiency at near-IR wavelengths, demonstrating the potential of MBE-grown NbN for realizing large arrays of on-chip SNSPDs and their integration with AlN-based $\chi^{(2)}$ quantum photonic circuits.

Superconducting nanowire single-photon detectors (SNSPDs)[1,2] have become an indispensable resource for a range of quantum and classical applications due to their high detection efficiency over a broad spectrum,[3–6] ultra-fast speed,[7,8] exceptional timing performance,[9–11] and ultra-low dark count noise.[12,13] Two categories of superconducting materials have so far been used for the fabrication of high-efficiency SNSPDs—poly-crystalline nitride and amorphous alloy superconductors. SNSPDs patterned from thin-film amorphous superconducting materials, such as WSi[3,14] and MoSi,[15–17] have exhibited excellent homogeneity over a large device area[18] due to the absence of grain boundaries. However, they require relatively low operation temperature and have lower ultimate counting rates, resulting from the longer hot spot relaxation time in comparison with the SNSPDs made from nitride superconductors, such as NbN[19–22] and NbTiN.[23–27] On the other hand, Nb(Ti)N-based detectors have shown relatively superior timing performance, demonstrating < 3 ps jitter measured with a short straight nanowire[10] and < 8 ps with a large-area meandered nanowire.[28] Despite these advantages, the homogeneity of Nb(Ti)N-SNSPDs is ultimately limited by the poly-crystalline nature of the Nb(Ti)N films, leading to non-uniform distribution of critical currents and limited fabrication yields in a large array of single-photon detectors required for future integrated quantum photonic circuits.

In this Letter, we demonstrate SNSPDs made from single-crystal NbN thin films grown by molecular beam epitaxy (MBE)[29] on nearly lattice-matched AlN-on-sapphire substrates. This substrate platform is attractive for the integration of SNSPDs with several other elements of nitride-based photonic integrated circuits.[30–34] The epitaxial NbN films exhibit a high degree of thickness uniformity and structural perfection owing to the 2D layer-by-layer growth unique to the MBE technique. The fabricated device consisting of 20 nm-wide and 6.3 nm-thick nanowire shows saturated internal efficiency at wavelengths of 780 nm and 1050 nm, while a further reduction in the achievable thin film thickness holds promise for saturating the efficiency at longer wavelengths with a more relaxed wire width. We expect that the MBE-NbN directly grown on the AlN-on-sapphire substrate shown here could provide a scalable material platform for realizing large arrays of on-chip SNSPDs and their integration with nitride-based photonic circuits.

As illustrated in Fig. 1, epitaxial NbN films are grown by radio frequency plasma-assisted MBE on a commercial 2 in.-diameter *c*-plane sapphire substrate with a 3 μm-thick AlN film grown by hydride vapor phase epitaxy (HVPE). A 240 nm-thick AlN film of Al-polar orientation is grown by MBE, followed by the growth of NbN as shown in Fig. 1(d). During the growth of the films, reactive nitrogen is

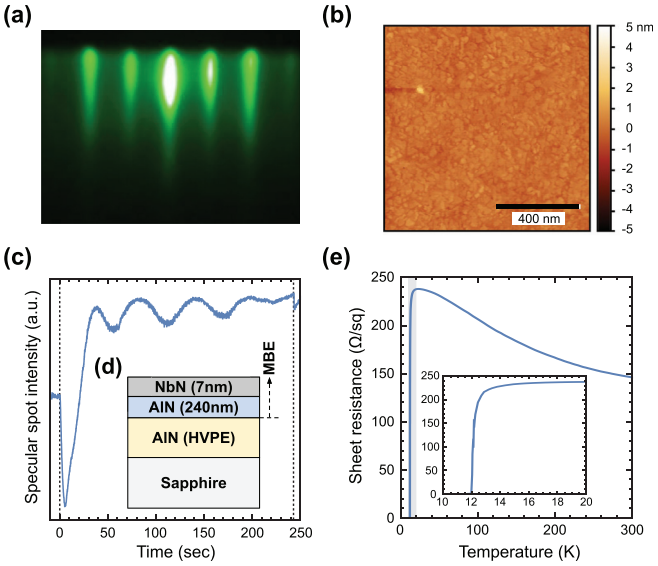

FIG. 1. (a) *In situ* RHEED pattern measured after the film growth demonstrating the epitaxial nature of the NbN film. The streakiness of the pattern evidences that the surface is effectively 2D. (b) AFM surface height map of the NbN thin film exhibiting R_{rms} = 0.29 nm. (c) RHEED intensity monitored throughout the NbN thin film growth. The exhibited oscillations of the specular spot brightness indicate the 2D layer-by-layer growth mode of NbN. (d) Cross-sectional sketch of the thin film layer structure. (e) Measured sheet resistance of the NbN thin film vs temperature with the inset showing the T_c value of 12.1 K.

generated using a radio frequency plasma source fed by ultrahigh-purity N_2 gas, which is further purified by an in-line purifier. Aluminum (99.9999% purity) is supplied using a Knudsen effusion cell. The Nb flux is generated using an *in situ* electron-beam evaporator source with 3N5-pure (excluding tantalum, Ta) Nb pellets in a tungsten hearth liner. The NbN films are grown at the temperature of 1100 °C, measured using a thermo-couple behind the substrate, and at a growth rate of approximately 1.0 nm/min.

The MBE film growth is monitored *in situ* using a reflection high-energy electron diffraction (RHEED) system operated at a voltage of 15 kV and a current of 1.5 A. Figure 1(a) shows sharp and streaky patterns formed by electron diffraction from the smooth surface of the NbN film, indicating the epitaxial nature of the single-crystal NbN film. As shown in Fig. 1(c), the *in situ* observation of oscillations of the RHEED intensity vs the growth time confirms that NbN grows in a 2D layer-by-layer growth mode on the AlN surface. The thicknesses of the NbN film and its native oxide layer are 6.3 nm and 1.2 nm, obtained by fitting the measurement data from x-ray reflectivity (XRR) with a Rigaku SmartLab diffractometer using CuKα1 radiation. Figure 1(b) shows the morphology of the NbN film surface characterized employing tapping mode atomic force microscopy (AFM); the root mean square roughness (R_{rms}) of the film surface is less than 0.3 nm within a scan size of 1 μm × 1 μm. In addition, the crystal orientation of NbN is determined using RHEED and x-ray diffraction (XRD), which indicates that cubic NbN grows with the {1 1 1} crystal axis aligned to the *c*-axis of AlN.

Figure 1(e) shows the temperature dependence of the sheet resistance of the MBE-NbN thin film with the inset showing a zoom-in view of the superconducting transition region. The transition temperature of the film is measured to be T_c = 12.1 K, defined as the temperature where the normal state resistance of the film drops to 50% of that measured at 20 K. This value is higher than the previous results of NbN[35] and NbTiN[36] thin films sputtered on AlN substrates for SNSPD fabrication. The high T_c value is also consistent with the significantly low resistivity of the film, which is calculated to be only ~100 $\mu\Omega \cdot$ cm obtained by multiplying the thickness with the room-temperature sheet resistance.

We fabricate SNSPD devices by patterning the MBE-NbN thin film. The nanowires are defined by the exposure of negative-tone 6% hydrogen silsesquioxane (HSQ) resist using 100 kV electron-beam lithography (Raith EBPG 5000+) and the subsequent development in 25% tetramethylammonium hydroxide (TMAH) for 2 min at room temperature. The HSQ resist is spun at the speed of 4000 rpm, resulting in an approximate thickness of 90 nm. In a second electron-beam lithography step, contact electrodes are defined using double-layer polymethyl methacrylate (PMMA) positive-tone resist. After the development in the mixture of methyl isobutyl ketone (MIBK) and isopropyl alcohol (IPA), we lift off the electron-beam evaporated 10 nm-thick Cr adhesion layer and 100 nm-thick Au in acetone overnight to form the contact pads. The HSQ nanowire pattern is then transferred to the NbN layer in a timed reactive-ion etching (RIE) step employing CF_4 chemistry and 50 W RF power. The HSQ resist is left on top of the NbN nanowires after fabrication, serving as a barrier to oxidation.

For initial tests, we fabricate short-nanowire detectors with widths ranging from 20 nm to 100 nm for comparison of the internal efficiencies. As shown in Figs. 2(a) and 2(b), the active detection parts of the devices are made of 20 μm-long straight nanowires, which are suitable for future waveguide integration. All the nanowires are serially connected to long 1 μm-wide meandered wires to prevent the detector latching at high bias currents. The sheet resistance of the devices is measured to be around 180 Ω/sq, which slightly increases compared to the value measured on the bare film prior to fabrication.

In order to characterize the optical response of the fabricated detectors, the detector chip containing multiple devices is mounted on a 3-axis stack of Attocube stages inside a closed-cycle refrigerator and cooled down to a base temperature of 1.7 K. Continuous wave (CW) laser light with varying wavelengths is attenuated to the single-photon level and sent to the detector chip via a standard telecommunication fiber (SMF-28) installed in the refrigerator. The detectors are flood-illuminated by fixing the fiber tip far away from the surface of the detector chip. We control the Attocube stages to move the detector chip at low temperature and make an electrical contact between the RF probes and the gold pads of the detectors. The RF probes are connected to a semi-rigid coaxial cable installed in the refrigerator, while the room-temperature end of the cable is attached to a bias-tee (Mini-Circuits ZFBT-6GW+) to separate the DC bias current and RF output pulses for the detectors. The bias current is supplied by a programmable sourcemeter (Keithley 2401) in conjunction with a low-pass filter (1 kHz cut-off frequency). The output pulses of the detectors are amplified by a low-noise RF amplifier (RF bay LNA-650) and sent to a 4 GHz oscilloscope for the pulse observation or a pulse counter (PicoQuant PicoHarp 300) for the photon counting measurement. Figure 2(c) shows a single-shot trace measurement of the output voltage pulse from the 20 nm-wide detector. The decay time constant extracted from the exponential fitting (red dashed line) is 5.4 ns, which

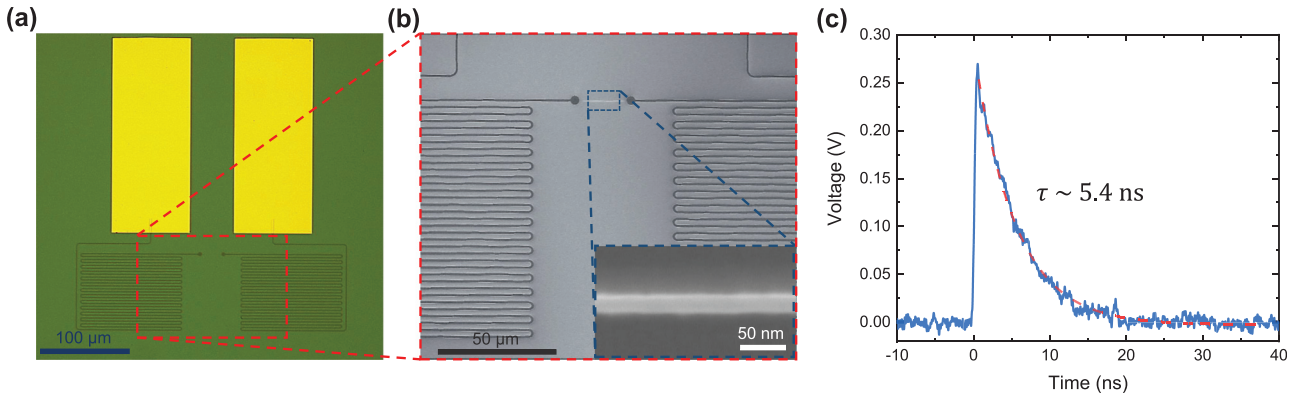

FIG. 2. (a) Optical micrograph image of the fabricated SNSPD device. (b) Close-up scanning electron micrograph (SEM) image of the active straight nanowire and the series inductor made of 1 μm-wide meandered wire. The inset shows the further zoom-in view of the 20 nm-wide straight nanowire. (c) Single-shot trace of output voltage pulses from the 20 nm-wide detector measured using a 4 GHz oscilloscope. The decay time constant (τ) extracted from an exponential fitting (red dashed line) is 5.4 ns.

translates into a sheet kinetic inductance of 24 pH/sq of the NbN film, assuming 50 Ω input impedance of the readout amplifier.

Figure 3 demonstrates the normalized photon counting rates (PCRs) as a function of the relative bias current to the switching current (I_{bias}/I_{SW}) for 20 nm-wide and 30 nm-wide nanowire detectors. I_{SW} values of the devices are measured to be 25.5 μA and 38.8 μA, respectively, indicating a critical current density of ~20 MA/cm^2. We also measure I_{SW} for wider nanowires (40–100 nm width), which show an excellent linear dependence on the wire width. The extrapolation of the data indicates a negligible "dead" width of the wires within the measurement errors, thereby confirming the absence of the edge damage effect during the fabrication process in contrast to the results reported by Charaev *et al.*[37] As expected, detectors made of narrower nanowires with reduced I_{SW} show better saturated internal efficiencies at a shorter wavelength. For the 20 nm-wide nanowire detector, we observe a clear saturation plateau at a wavelength of 780 nm, while the

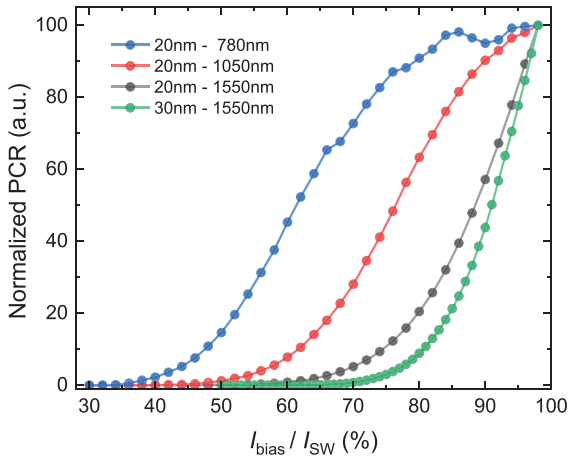

FIG. 3. Normalized photon counting rates (PCRs) vs the relative bias current (I_{bias}/I_{SW}) measured with the 20 nm-wide and 30 nm-wide nanowire detectors for varying wavelengths of photons. I_{SW} values of the nanowires are measured to be 25.5 μA and 38.8 μA, respectively.

efficiency is only nearly saturated at a wavelength of 1050 nm. The minor fluctuation in the curve corresponding to a wavelength of 780 nm is due to the polarization instability of the laser since the photon absorption of the nanowire is significantly dependent on the polarization status of the incident photons. Neither the 20 nm-wide nor the 30 nm-wide nanowires show saturation behavior at a wavelength of 1550 nm. We attribute the inefficiency of the detectors to the possibly larger diffusion coefficient (D) of the single-crystal MBE-NbN material in comparison with sputtered[19] or atomic-layer-deposited (ALD)[22,38] poly-crystal NbN that has been utilized for the fabrication of high-efficiency SNSPDs. As indicated by the theory of photon detection mechanism based on hot-spot and vortex assistance,[39,40] a larger D allows faster diffusion of electrons, which favors a relatively low "temperature" of the hot electrons, because the energy of absorbed photons is confined to a relatively large volume at the initial stage of hot-spot formation. This, in turn, reduces the internal efficiency of the detectors owing to the decreased probability of superconducting state collapse under the assistance of the vortex-antivortex pair, which nucleates in the region with a less-suppressed superconducting order parameter. However, we expect that by further reducing the MBE-NbN film thickness down to 2–3 nm, this effect could be compensated, and saturated efficiency can be obtained at longer wavelengths with relaxed nanowire widths up to > 100 nm, as recently demonstrated with ultra-thin WSi and MoSi films.[41,42] The growth of high-crystalline-quality NbN films of 3 nm thick or less is achievable by MBE although a method to protect such thin films from oxidation upon exposure to the ambient air is necessary and under investigation. Future work will explore the suitability of such ultra-thin films for SNSPDs.

In summary, we have demonstrated the first SNSPDs patterned from MBE-grown single-crystal NbN thin films on AlN substrates. The 20 nm-wide SNSPDs show saturated internal efficiency at the wavelength of 780 nm and near-saturation at 1050 nm. We expect that single-crystal MBE-NbN could address the limited fabrication yield problem, which conventional poly-crystalline-Nb(Ti)N detectors suffer from, by removing the grain boundaries and thus reducing the defect area in the film to the minimum level. It is also worth mentioning that the AlN-on-sapphire substrate, which the epitaxial growth of

NbN relies on, is particularly attractive due to its potential of the on-chip integration of SNSPDs with versatile AlN nanophotonic circuits. The excellent optical functionalities of AlN, such as strong $\chi^{(2)}/\chi^{(3)}$ nonlinearity[43] and large electro-optic effect,[44,45] render NbN on AlN-on-sapphire a very attractive material platform for realizing fully integrated quantum photonic circuits with the generation, routing, active manipulation, and the final detection of single photons on a single chip.

AUTHORS' CONTRIBUTIONS

R.C. and J.W. contributed equally to this work.

This project was funded by the Office of Naval Research Grant (Nos. N00014–20-1–2126 and N00014–20-1–2176) monitored by Dr. Paul Maki. D.J. acknowledges funding support from NSF RAISE TAQ Award No. 1839196 monitored by Dr. D. Dagenais. H.X.T. acknowledges funding support from the DARPA DETECT program through an ARO Grant (No: W911NF-16–2-0151), NSF EFRI Grant (No. EFMA-1640959), and the Packard Foundation. The authors would like to thank Sean Rinehart, Kelly Woods, Dr. Yong Sun, and Dr. Michael Rooks at Yale University for their assistance provided in the device fabrication and Dr. Scott Katzer and Dr. David Meyer at the Naval Research Laboratory for useful discussions. The epitaxial growth was performed at Cornell University, and material characterization used resources made available by NSF CCMR MRSEC Award No. 1719875. The fabrication of the devices was done at the Yale School of Engineering and Applied Science (SEAS) Cleanroom and the Yale Institute for Nanoscience and Quantum Engineering (YINQE).

DATA AVAILABILITY

The data that support the findings of this study are available from the corresponding author upon reasonable request.

REFERENCES

[1]G. Gol'Tsman, O. Okunev, G. Chulkova, A. Lipatov, A. Semenov, K. Smirnov, B. Voronov, A. Dzardanov, C. Williams, and R. Sobolewski, "Picosecond superconducting single-photon optical detector," Appl. Phys. Lett. **79**, 705 (2001).
[2]R. H. Hadfield, "Single-photon detectors for optical quantum information applications," Nat. Photonics **3**, 696 (2009).
[3]F. Marsili, V. B. Verma, J. A. Stern, S. Harrington, A. E. Lita, T. Gerrits, I. Vayshenker, B. Baek, M. D. Shaw, R. P. Mirin, and S. W. Nam, "Detecting single infrared photons with 93% system efficiency," Nat. Photonics **7**, 210 (2013).
[4]V. Verma, A. Lita, B. Korzh, E. Wollman, M. Shaw, R. Mirin, and S. Nam, "Towards single-photon spectroscopy in the mid-infrared using superconducting nanowire single-photon detectors," Proc. SPIE **10978**, 109780N (2019).
[5]F. Marsili, F. Bellei, F. Najafi, A. Dane, E. Dauler, R. J. Molnar, and K. K. Berggren, "Efficient single photon detection from 500 nm to 5 μm wavelength," Nano Lett. **12**, 4799 (2012).
[6]D. V. Reddy, A. E. Lita, S. W. Nam, R. P. Mirin, and V. B. Verma, "Achieving 98% system efficiency at 1550 nm in superconducting nanowire single photon detectors," in *Rochester Conference on Coherence and Quantum Optics (CQO-11)* (OSA, 2019).
[7]J. Münzberg, A. Vetter, F. Beutel, W. Hartmann, S. Ferrari, W. H. Pernice, and C. Rockstuhl, "Superconducting nanowire single-photon detector implemented in a 2D photonic crystal cavity," Optica **5**, 658 (2018).
[8]W. Zhang, J. Huang, C. Zhang, L. You, C. Lv, L. Zhang, H. Li, Z. Wang, and X. Xie, "A 16-pixel interleaved superconducting nanowire single-photon detector array with a maximum count rate exceeding 1.5 GHz," IEEE Trans. Appl. Supercond. **29**, 1 (2019).
[9]I. E. Zadeh, J. W. Los, R. Gourgues, G. Bulgarini, S. M. Dobrovolskiy, V. Zwiller, and S. N. Dorenbos, "A single-photon detector with high efficiency and sub-10 ps time resolution," preprint arXiv:1801.06574 (2018).
[10]B. Korzh, Q.-Y. Zhao, J. P. Allmaras, S. Frasca, T. M. Autry, E. A. Bersin, A. D. Beyer, R. M. Briggs, B. Bumble, M. Colangelo, G. M. Crouch, A. E. Dane, T. Gerrits, A. E. Lita, F. Marsili, G. Moody, C. Peña, E. Ramirez, J. D. Rezac, N. Sinclair, M. J. Stevens, A. E. Velasco, V. B. Verma, E. E. Wollman, S. Xie, D. Zhu, P. D. Hale, M. Spiropulu, K. L. Silverman, R. P. Mirin, S. W. Nam, A. G. Kozorezov, M. D. Shaw, and K. K. Berggren, "Demonstration of sub-3 ps temporal resolution with a superconducting nanowire single-photon detector," Nat. Photonics **14**, 250 (2020).
[11]I. E. Zadeh, J. W. Los, R. Gourgues, J. Chang, A. W. Elshaari, J. Zichi, Y. J. van Staaden, J. Swens, N. Kalhor, A. Guardiani *et al.*, "A platform for high performance photon correlation measurements," preprint arXiv:2003.09916 (2020).
[12]C. Schuck, W. H. P. Pernice, and H. X. Tang, "Waveguide integrated low noise NbTiN nanowire single-photon detectors with milli-Hz dark count rate," Sci. Rep. **3**, 1893 (2013).
[13]H. Shibata, K. Shimizu, H. Takesue, and Y. Tokura, "Ultimate low system dark-count rate for superconducting nanowire single-photon detector," Opt. Lett. **40**, 3428 (2015).
[14]B. Baek, A. E. Lita, V. Verma, and S. W. Nam, "Superconducting a-W_xSi_{1-x} nanowire single-photon detector with saturated internal quantum efficiency from visible to 1850 nm," Appl. Phys. Lett. **98**, 251105 (2011).
[15]M. Caloz, M. Perrenoud, C. Autebert, B. Korzh, M. Weiss, C. Schönenberger, R. J. Warburton, H. Zbinden, and F. Bussières, "High-detection efficiency and low-timing jitter with amorphous superconducting nanowire single-photon detectors," Appl. Phys. Lett. **112**, 061103 (2018).
[16]Y. P. Korneeva, M. Y. Mikhailov, Y. P. Pershin, N. Manova, A. Divochiy, Y. B. Vakhtomin, A. Korneev, K. Smirnov, A. Sivakov, A. Y. Devizenko *et al.*, "Superconducting single-photon detector made of MoSi film," Supercond. Sci. Technol. **27**, 095012 (2014).
[17]J. Li, R. A. Kirkwood, L. J. Baker, D. Bosworth, K. Erotokritou, A. Banerjee, R. M. Heath, C. M. Natarajan, Z. H. Barber, M. Sorel *et al.*, "Nano-optical single-photon response mapping of waveguide integrated molybdenum silicide (MoSi) superconducting nanowires," Opt. Express **24**, 13931 (2016).
[18]E. E. Wollman, V. B. Verma, A. E. Lita, W. H. Farr, M. D. Shaw, R. P. Mirin, and S. W. Nam, "Kilopixel array of superconducting nanowire single-photon detectors," Opt. Express **27**, 35279 (2019).
[19]W. Zhang, L. You, H. Li, J. Huang, C. Lv, L. Zhang, X. Liu, J. Wu, Z. Wang, and X. Xie, "NbN superconducting nanowire single photon detector with efficiency over 90% at 1550 nm wavelength operational at compact cryocooler temperature," Sci. China: Phys., Mech. Astron. **60**, 120314 (2017).
[20]O. Kahl, S. Ferrari, V. Kovalyuk, G. N. Goltsman, A. Korneev, and W. H. Pernice, "Waveguide integrated superconducting single-photon detectors with high internal quantum efficiency at telecom wavelengths," Sci. Rep. **5**, 10941 (2015).
[21]W. Pernice, C. Schuck, O. Minaeva, M. Li, G. Goltsman, A. Sergienko, and H. Tang, "High-speed and high-efficiency travelling wave single-photon detectors embedded in nanophotonic circuits," Nat. Commun. **3**, 1325 (2012).
[22]R. Cheng, S. Wang, and H. X. Tang, "Superconducting nanowire single-photon detectors fabricated from atomic-layer-deposited NbN," Appl. Phys. Lett. **115**, 241101 (2019).
[23]I. Esmaeil Zadeh, J. W. Los, R. B. Gourgues, V. Steinmetz, G. Bulgarini, S. M. Dobrovolskiy, V. Zwiller, and S. N. Dorenbos, "Single-photon detectors combining high efficiency, high detection rates, and ultra-high timing resolution," APL Photonics **2**, 111301 (2017).
[24]R. Cheng, M. Poot, X. Guo, L. Fan, and H. X. Tang, "Large-area superconducting nanowire single-photon detector with double-stage avalanche structure," IEEE Trans. Appl. Supercond. **27**, 1 (2017).
[25]R. Cheng, X. Guo, X. Ma, L. Fan, K. Y. Fong, M. Poot, and H. X. Tang, "Self-aligned multi-channel superconducting nanowire single-photon detectors," Opt. Express **24**, 27070 (2016).
[26]S. Miki, M. Yabuno, T. Yamashita, and H. Terai, "Stable, high-performance operation of a fiber-coupled superconducting nanowire avalanche photon detector," Opt. Express **25**, 6796 (2017).
[27]H. Machhadani, J. Zichi, C. Bougerol, S. Lequien, J.-L. Thomassin, N. Mollard, A. Mukhtarova, V. Zwiller, J.-M. Gérard, and E. Monroy, "Improvement of the

critical temperature of NbTiN films on III-nitride substrates," Superconductor Sci. Technol. **32**, 035008 (2019).
[28]I. E. Zadeh, J. W. N. Los, R. B. M. Gourgues, J. Chang, A. W. Elshaari, J. R. Zichi, Y. J. van Staaden, J. P. E. Swens, N. Kalhor, A. Guardiani, Y. Meng, K. Zou, S. Dobrovolskiy, A. W. Fognini, D. R. Schaart, D. Dalacu, P. J. Poole, M. E. Reimer, X. Hu, S. F. Pereira, V. Zwiller, and S. N. Dorenbos, "Efficient single-photon detection with 7.7 ps time resolution for photon correlation measurements," ACS Photonics **7**, 1780 (2020).
[29]R. Yan, G. Khalsa, S. Vishwanath, Y. Han, J. Wright, S. Rouvimov, D. S. Katzer, N. Nepal, B. P. Downey, D. A. Muller, H. G. Xing, D. J. Meyer, and D. Jena, "GaN/NbN epitaxial semiconductor/superconductor heterostructures," Nature **555**, 183 (2018).
[30]S. Ferrari, C. Schuck, and W. Pernice, "Waveguide-integrated superconducting nanowire single-photon detectors," Nanophotonics **7**, 1725 (2018).
[31]R. Cheng, C.-L. Zou, X. Guo, S. Wang, X. Han, and H. X. Tang, "Broadband on-chip single-photon spectrometer," Nat. Commun. **10**, 1 (2019).
[32]A. Gaggero, F. Martini, F. Mattioli, F. Chiarello, R. Cernansky, A. Politi, and R. Leoni, "Amplitude-multiplexed readout of single photon detectors based on superconducting nanowires," Optica **6**, 823 (2019).
[33]F. Najafi, J. Mower, N. C. Harris, F. Bellei, A. Dane, C. Lee, X. Hu, P. Kharel, F. Marsili, S. Assefa, K. K. Berggren, and D. Englund, "On-chip detection of non-classical light by scalable integration of single-photon detectors," Nat. Commun. **6**, 5873 (2015).
[34]R. Cheng, S. Wang, C.-L. Zou, and H. Tang, "Design of micron-long superconducting nanowire perfect absorber for efficient high speed single-photon detection," Photonics Res. **8**, 1260 (2020).
[35]D. Zhu, H. Choi, T.-J. Lu, Q. Zhao, A. Dane, F. Najafi, D. R. Englund, and K. K. Berggren, "Superconducting nanowire single-photon detector on aluminum nitride," in *Conference on Lasers and Electro-Optics* (OSA, 2016).
[36]S. Steinhauer, L. Yang, S. Gyger, T. Lettner, C. Errando-Herranz, K. D. Jöns, M. A. Baghban, K. Gallo, J. Zichi, and V. Zwiller, "NbTiN thin films for superconducting photon detectors on photonic and two-dimensional materials," Appl. Phys. Lett. **116**, 171101 (2020).
[37]I. Charaev, T. Silbernagel, B. Bachowsky, A. Kuzmin, S. Doerner, K. Ilin, A. Semenov, D. Roditchev, D. Y. Vodolazov, and M. Siegel, "Proximity effect model of ultranarrow NbN strips," Phys. Rev. B **96**, 184517 (2017).
[38]A. A. Sayem, R. Cheng, S. Wang, and H. X. Tang, "Lithium-niobate-on-insulator waveguide-integrated superconducting nanowire single-photon detectors," Appl. Phys. Lett. **116**, 151102 (2020).
[39]A. N. Zotova and D. Y. Vodolazov, "Photon detection by current-carrying superconducting film: A time-dependent Ginzburg-Landau approach," Phys. Rev. B **85**, 024509 (2012).
[40]D. Vodolazov, "Single-photon detection by a dirty current-carrying superconducting strip based on the kinetic-equation approach," Phys. Rev. Appl. **7**, 034014 (2017).
[41]I. Charaev, Y. Morimoto, A. Dane, A. Agarwal, M. Colangelo, and K. K. Berggren, "Large-area microwire MoSi single-photon detectors at 1550 nm wavelength," Appl. Phys. Lett. **116**, 242603 (2020).
[42]J. Chiles, S. M. Buckley, A. Lita, V. B. Verma, J. Allmaras, B. Korzh, M. D. Shaw, J. M. Shainline, R. P. Mirin, and S. W. Nam, "Superconducting microwire detectors based on WSi with single-photon sensitivity in the near-infrared," Appl. Phys. Lett. **116**, 242602 (2020).
[43]X. Guo, C.-L. Zou, C. Schuck, H. Jung, R. Cheng, and H. X. Tang, "Parametric down-conversion photon-pair source on a nanophotonic chip," Light: Sci. Appl. **6**, e16249 (2017).
[44]L. Fan, C.-L. Zou, R. Cheng, X. Guo, X. Han, Z. Gong, S. Wang, and H. X. Tang, "Superconducting cavity electro-optics: A platform for coherent photon conversion between superconducting and photonic circuits," Sci. Adv. **4**, eaar4994 (2018).
[45]C. Xiong, W. H. P. Pernice, X. Sun, C. Schuck, K. Y. Fong, and H. X. Tang, "Aluminum nitride as a new material for chip-scale optomechanics and nonlinear optics," New J. Phys. **14**, 095014 (2012).